

# Temperature dependence of ultrafast photoinduced ring-opening and -closure reactions of spironaphthooxazine in crystalline phase

Mototsugu Suzuki, Tsuyoshi Asahi\*, Hiroshi Masuhara\*\*

*Department of Applied Physics, Osaka University, Suita, Osaka 565-0871, Japan*

Available online 2 December 2005

## Abstract

To investigate the dynamics of photoinduced ring-opening and -closure reactions in crystalline phase, we measured transient absorption spectra of spironaphthooxazine microcrystalline powder by femtosecond diffuse reflectance spectroscopy and examined their temperature dependence. The lifetimes of the excited state of the spiro form and the subsequent non-planar open form were about 3 ps and 3 ns at room temperature, respectively. The temperature dependence of their decay constant showed the Arrhenius type behavior and the activation energy of the ring-opening and -closure reactions are estimated to 7 and 12 kJ mol<sup>-1</sup>, respectively. The yield of the non-planar open form became smaller at lower temperature, and it was zero below about 140 K. The experimental results and kinetic analysis indicate that a short-lived species having a molecular conformation different from the non-planar form should be considered as an intermediate in the ring-opening reaction.

© 2005 Elsevier B.V. All rights reserved.

**Keywords:** Photochromism; Spirooxazine; Solid state reaction; Reaction dynamics; Transient absorption spectroscopy; Temperature dependence

## 1. Introduction

Spirooxazine is one of the most fatigue-resistant in photochromic compounds, and the photochromic feature has been studied from the viewpoints not only of its applications to optical memories and switches but also of fundamental elucidation of photochemical reaction [1–6]. Upon UV light excitation, spiro carbon–oxygen (C–O) bond of the colorless spiro form breaks and the subsequent isomerization leads to colored open isomers called photomerocyanines (PMCs), as shown in Scheme 1 [1–3]. The PMCs return back to the initial spiro form thermally or photochemically. The primary photocoloration process have been investigated intensely in solution systems, and the structure and electronic nature of a non-planar open form just after C–O bond cleavage are one of the most interesting topics [1–6]. Although several works with picosecond and femtosecond pump-probe techniques were reported, the detail reaction dynamics of the non-planar open form has not been clear yet. This will be owing to very rapid isomerization into planar forms of PMC. It was reported for several spiropyran and spirooxazine compounds that characteristic absorption spectra of planar PMCs grew up in

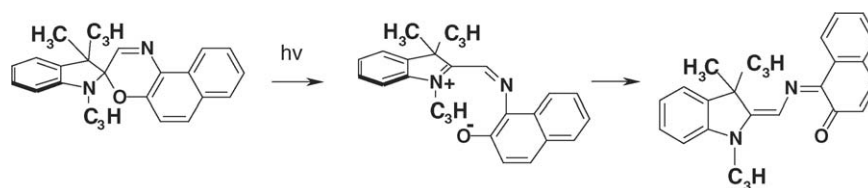
a few ps after ps or fs laser excitation [4–6]. However, the conformational change into a planar form occurs in the same time scale to the C–O bond cleavage reaction in the singlet excited (S<sub>1</sub>) state of the closed form.

In crystalline phase of spironaphthooxazine (1,3-dihydro-1,3,3-trimethylspiro[2H-indole-2,3'-[3H]naphth[2,1-b][1,4]oxazine], SNO), a non-planar open form of lives in a nanosecond time scale, which was confirmed directly by femtosecond transient absorption measurement [7–11]. The non-planar form is generated in 5 ps after excitation, and it returns back to the ground state spiro-isomer in 3 ns, not leading to trans-planar PMCs. The similar photochemical reaction dynamics was observed for several spiropyran and spirooxazine compounds, and the lifetime of the non-planar form was influenced by the molecular and crystalline structures [9]. In crystalline phase, any structural changes of molecules are strongly restricted in a lattice environment, so we can confirm clearly a non-planar nature of the photoprimary product. Thus, the investigation of ultrafast dynamics of crystalline systems brings more detailed information on the primary process of the photochromic reaction. Furthermore, we have found recently that the microcrystalline powder of SNO exhibits photocoloration exclusively by intense femtosecond laser excitation. We consider the photocoloration mechanism from the viewpoint of time-dependent density of short-lived transient species, and proposed that cooperative interactions of excited

\* Corresponding author. Tel.: +81 6 6879 7838.

\*\* Corresponding author. Tel.: +81 6 6879 7837.

E-mail addresses: [asahi@ap.eng.osaka-u.ac.jp](mailto:asahi@ap.eng.osaka-u.ac.jp) (T. Asahi), [masuhara@ap.eng.osaka-u.ac.jp](mailto:masuhara@ap.eng.osaka-u.ac.jp) (H. Masuhara).



Scheme 1.

states and non-planar open forms play an important role in the femtosecond laser-induced photochromism [7–10]. The elucidation of the primary photochemical reaction dynamics is essential also for understanding this femtosecond laser-induced photocoloration phenomenon.

In this work, we have measured femtosecond transient absorption spectra of SNO microcrystalline powder at various temperatures, and investigated the temperature dependence of photoinduced ring-opening and -closure reaction dynamics. The lifetimes of the  $S_1$  state and the non-planar open form became longer at lower temperatures, which means that both the C–O bond breaking in the  $S_1$  state and ring-closure reaction of the non-planar open form are thermally activated events and need a local and transient lattice deformation. We found also that the yield of the non-planar open form decreased with lowering temperature. On the basis of these results, we will discuss the dynamics of photoinduced ring-opening and -closure reactions and propose the photo isomerization mechanism in the crystalline phase.

## 2. Experimental

### 2.1. Materials

SNO (Aldrich) was recrystallized from hexane (spectral grade, Nacalai Tesque) in dark and sublimated under vacuum. The averaged particle size of the powder samples was about several tens of  $\mu\text{m}$ . The powder sample was contained in quartz cells with 1 mm optical path length and degassed with a vacuum pump.

### 2.2. Femtosecond transient absorption spectrum measurement

The details of our femtosecond diffuse reflectance spectroscopic system have been reported elsewhere [12,13]. The fundamental output from a regenerative femtosecond Ti:sapphire amplifier was frequency doubled (390 nm) and used as a femtosecond excitation pulse. The residual of the fundamental output was focused into a 1 cm quartz cell containing  $\text{H}_2\text{O}$  in order to generate a white-light continuum as a probe light. The transient absorption intensity was displayed as percentage absorption (%absorption), given by  $\% \text{absorption} = 100 \times (1 - R/R_0)$ , where  $R$  and  $R_0$  represent the intensity of the diffuse reflected white-light continuum of a probe pulse with and without excitation, respectively. The excitation intensity was adjusted to be less than  $0.9 \text{ mJ/cm}^2$ , under which any long-lived photoproducts

was not observed after 100 shots of excitation pulses in the temperature range from 208 to 367 K. The spectral data at one delay time were measured several times changing the position of samples every 50 laser shots. At the temperature below 200 K, the sample position was changed after every one measurement and the data was averaged, because a photocoloration was detected after 50 laser shots.

The sample temperature was controlled in the range from 190 to 363 K by placing the sample in a Dewar vessel. When the sample was set to lower than the room temperature, the vessel was contained with ethanol cooled by mixing liquid nitrogen, and when above room temperatures, it was with water heated with a tube heater.

## 3. Results and discussion

### 3.1. Transient absorption spectra and their temporal profiles

As representative examples, the transient absorption spectra and their time profiles at 363 and 168 K are shown in Figs. 1 and 2. We have already reported that a transient absorption spectrum with a peak at 500 nm and a plateau from 600 to 800 nm was observed just after excitation at 295 K and can be assigned to the  $S_n$ – $S_1$  absorption band of the spiro form [7,9–11]. The subsequent absorption spectrum with two peaks at 480 and 740 nm remained in a nanosecond time scale and it was assigned to a non-planar open form. Based on the results, we assign transient absorption spectra at various temperatures.

At 363 K, an absorption band with a peak at 500 nm and a broad one around 740 nm are observed immediately after excitation. After the decay of the band at 500 nm in 4 ps, two broad bands at 460 and 760 nm remain. Analyzing the temporal profiles of the absorption at 500 and 740 nm, the lifetime ( $\tau_{S_1}$ ) of the  $S_1$  state and that ( $\tau_{\text{cis}}$ ) of the non-planar open form are estimated to be 1.5 and 600 ps, respectively. On the other hand, at 168 K an absorption peak at 500 nm was observed immediately after excitation as well as at the room and high temperature; however, the subsequent transient absorption spectrum with a peak around 740 nm is less striking. From the temporal profiles of the transient absorption, the decay time constant of the  $S_1$  state of the spiro form is 22 ps and that of the non-planar open form constant is longer than 20 ns. These results indicate that at a low temperature the yield of the non-planar open form is lower than that at the room temperature, although non-planar open form hardly reverts to the ground state of the spiro form.

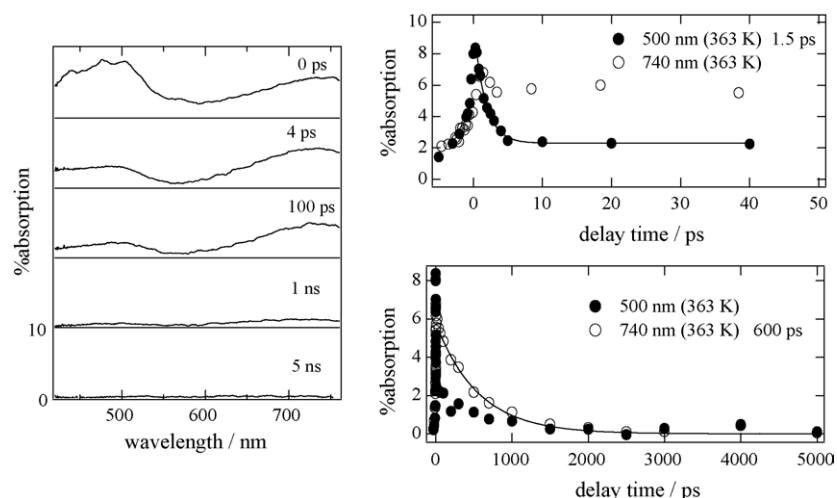


Fig. 1. Transient absorption spectra and the temporal profiles at 500 nm (●) and 740 nm (○) for SNO microcrystalline powder at 363 K. The decay time constants at 500 and 740 nm are 1.5 and 600 ps, respectively.

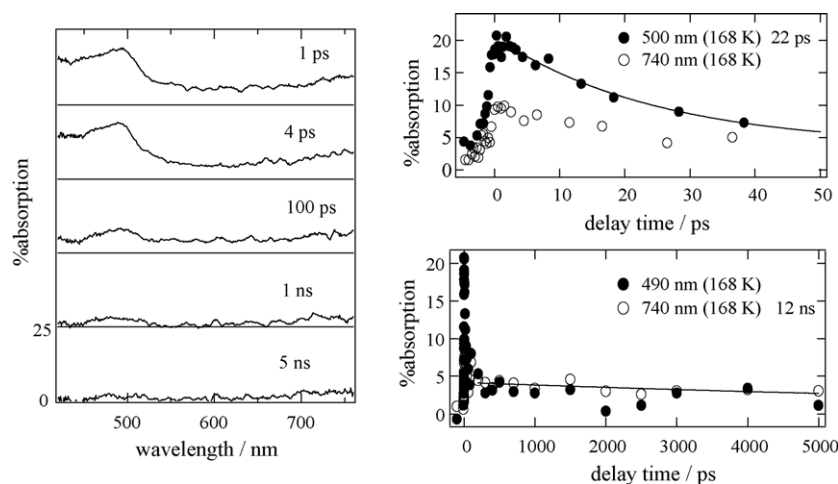


Fig. 2. Transient absorption spectra and the temporal profiles at 490 nm (●) and 740 nm (○) for SNO microcrystalline powder at 168 K. The decay time constants at 490 and 740 nm are 22 and 12 ns, respectively.

### 3.2. Temperature dependence of the rate constants of ring-opening and -closure reactions

The lifetimes of the  $S_1$  state and the non-planar open form are summarized in Table 1. The Arrhenius plots of the rate constants,  $k_{S1}$  and  $k_{cis}$ , which are defined, respectively, as  $1/\tau_{S1}$  and  $1/\tau_{cis}$ , are shown in Fig. 3. It is clear that the ring-opening reaction in the  $S_1$  state and the ring-closure one of the non-planar form show the Arrhenius type temperature dependence (Eq. (1)).

$$\ln k = \ln A - \frac{E}{RT} \quad (1)$$

We estimated the frequency factor and the activation energy for the decay of the  $S_1$  state to be  $A_{S1} = 5.3 \times 10^{12} \text{ s}^{-1}$  and  $E_{S1} = 7 \text{ kJ mol}^{-1}$ , and those of the non-planar form to be  $A_{cis} = 5.0 \times 10^{10} \text{ s}^{-1}$  and  $E_{cis} = 12 \text{ kJ mol}^{-1}$ , respectively. The result indicates that the ring-opening reaction does not occur in orthogonal parent geometry of the indolino and oxazine chromophors and that it will be coupled to both the intramolecular

vibrational motions such as twisting around the spiro carbon, and lattice deformation. Moreover, it is demonstrated that the activation energy of the ring-closure process is larger than that of the ring-opening reaction in the  $S_1$  state.

Table 1  
Lifetimes of the excited state of the spiro form,  $\tau_{S1}$ , and the non-planar open form,  $\tau_{cis}$ , of SNO microcrystalline powder

Temperature (K)	$\tau_{S1}$ (ps)	$\tau_{cis}$ (ns)
363	1.5	0.6
295	3.1	3.0
283	3.3	<sup>a</sup>
275	4.3	4.6
264	<sup>a</sup>	5.0
253	5.2	<sup>a</sup>
223	9.0	9.0
208	10	<sup>a</sup>
193	14	>20
168	22	<sup>a</sup>
77	140 and >5 ns	–

<sup>a</sup> No data.

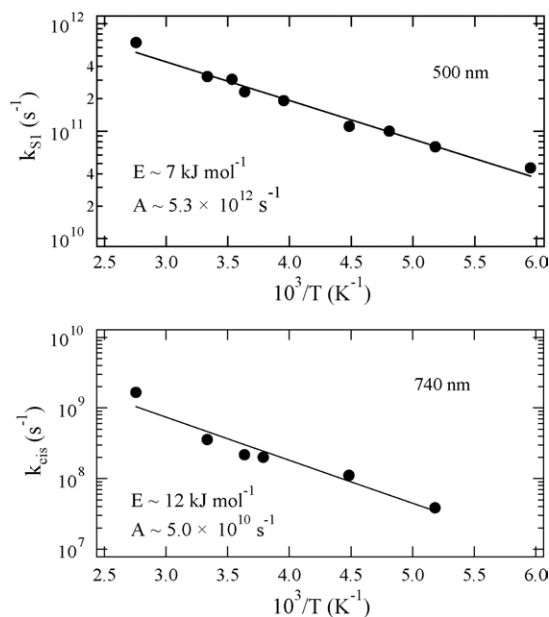


Fig. 3. Temperature dependence of  $k_{S1}$  and  $k_{cis}$  (filled circles) and Arrhenius analysis (solid lines) using Eq. (1). Fitting parameters,  $E$  and  $A$ , are shown in the figures.

Tamai et al. reported that the ring-opening reaction in the  $S_1$  state does not need any activation energy in solution and does not depend on solvent viscosity [5,6]. Molecules in fluid solution and rigid glass matrix can change their conformation easily owing to enough free volume [1–3,14]. On the other hand, molecular conformation changes are hindered strongly by the neighboring molecules in crystalline phase, and some structural changes leading to its open forms will be restricted by a local free volume which is determined by molecular packing manner in the crystal. Consequently, the ring-opening reaction of SNO crystal is slower compared to a solution system and large activation energy ( $7 \text{ kJ mol}^{-1}$ ) is necessary for C–O bond breaking. Indeed, we have recently reported that the ultrafast dynamics of the ring-opening and -closure reactions is sensitive to the crystalline structure. The lifetime of the  $S_1$  state and the non-planar open form are quite different between SNO and its chloro-substituted compound (5-chloro-1,3-dihydro-1,3,3-trimethylspiro[2H-indole-2,3'-[3H]naphth[2,1-b][1,4]oxazine], Cl-SNO) in crystalline phase at room temperature, while their photochromic dynamics in solution is almost the same to each other. [11]. Furthermore, Cl-SNO microcrystal showed a temperature independent lifetime of the  $S_1$  state; it was 1 ps both at 295 and 77 K.

### 3.3. Temperature dependence of the yield ratio of the non-planar open form

As mentioned above, the yield of the non-planar open form is dependent on the temperature. To consider the dependence quantitatively, we estimated the relative yield, Yield, from Eq. (2)

$$\text{Yield} = \frac{\% \text{Abs}(740 \text{ nm}; 50 \text{ ps})}{\% \text{Abs}(500 \text{ nm}; 0 \text{ ps})} \quad (2)$$

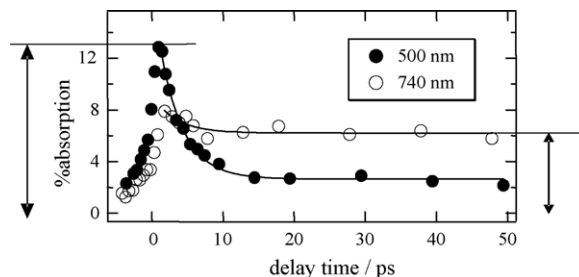


Fig. 4. Schematic illustration for analyzing the relative yield of the non-planar open form.

where  $\% \text{Abs}(\lambda; t)$  means the transient absorption at a wavelength  $\lambda$  and at a delay time  $t$  (see Fig. 4). On the base of the transient absorption spectra and their temporal profiles, we can set  $\% \text{Abs}(\lambda; t)$  to be the sum of the contributions of the  $S_1$  state and the non-planar open form, as shown by Eq. (3).

$$\% \text{Abs}(\lambda; t) = \varepsilon_{S1,\lambda} [S1] + \varepsilon_{cis,\lambda} [cis] \quad (3)$$

where  $\varepsilon_{S1,\lambda}$  and  $\varepsilon_{cis,\lambda}$  are absorption coefficients of the  $S_1$  state of the spiro form and the non-planar open form at a wavelength  $\lambda$ , respectively.  $[S1]$  and  $[cis]$  are the densities of the  $S_1$  state of the spiro form and the non-planar open form. As shown in Table 1, on the other hand,  $\tau_{S1}$  is shorter than 25 ps and  $\tau_{cis}$  is longer than 600 ps in the temperature range examined here. Then, when assuming the first-order kinetics and using the reaction yield,  $\Phi$ ,  $\% \text{Abs}(\lambda; t)$  at delay times less than 50 ps can be presented by the following equation.

$$\% \text{Abs}(\lambda; t) = [S1]_0 \left[ \Phi \varepsilon_{cis,\lambda} + (\varepsilon_{S1,\lambda} - \Phi \varepsilon_{cis,\lambda}) \exp\left(\frac{-t}{\tau_{S1}}\right) \right] \quad (4)$$

where  $[S1]_0$  the initial density of the  $S_1$  state. Because  $\exp(-t/\tau_{S1})$  is approximately zero at  $t = 50$  ps, we obtained the relation between Yield and  $\Phi$  as the following:

$$\text{Yield} = \left( \frac{\varepsilon_{cis,740 \text{ nm}}}{\varepsilon_{S1,500 \text{ nm}}} \right) \Phi \quad (5)$$

The temperature dependence of Yield is shown in Fig. 5. Since absorption coefficient will not vary drastically in the examined temperature range, the dependence means that the yield of the non-planar open form decreases linearly with decreasing temperature and the non-planar open form is not generated below

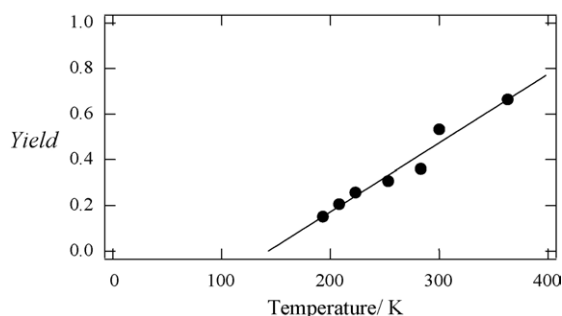


Fig. 5. Temperature dependence of relative yield, Yield, of the non-planar open form.

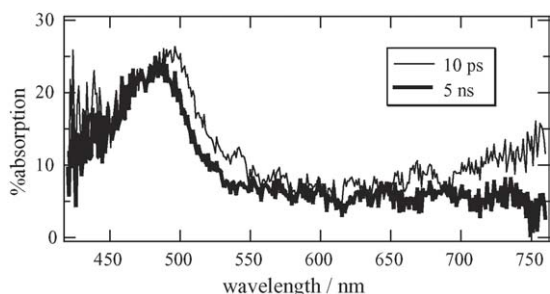


Fig. 6. Transient absorption spectra of SNO microcrystalline powder at 77 K.

140 K. This result is consistent with the transient absorption measurement at 77 K. As shown in Fig. 6, transient absorption spectrum with a peak around 500 nm was observed, while any characteristic band of the non-planar form absorption at 740 nm was not even at 5 ns after excitation.

### 3.4. The mechanism of the ring-opening reaction

The above results demonstrate that the decay processes both of the  $S_1$  state and the non-planar open form need thermal activation and that the former lifetime is much shorter than the latter one in the temperature from 160 to 360 K. On the contrary, the yield of the non-planar open form decreases drastically at lower temperatures. These temperature dependences indicate that only a part of the  $S_1$  states changes into the non-planar open form. We here consider the following two-reaction mechanism as the photoinduced ring-opening reaction. In *model A*, we take account of an intermediate species (X) from the  $S_1$  state to the non-planar open form, and in *model B* a rapid non-radiative relaxation pathway to the ground state of the spiro form. A schematic illustration of the reaction potential surface for each reaction mechanism is presented in Figs. 7 and 8, respectively. The horizontal axis of the potential energy curve represents the degree of the molecular

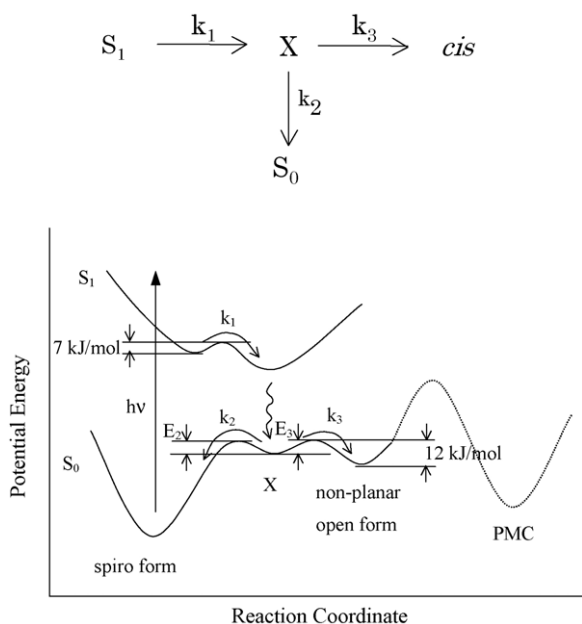


Fig. 7. Scheme and potential curve for the ring-opening reaction according to model A (see text).

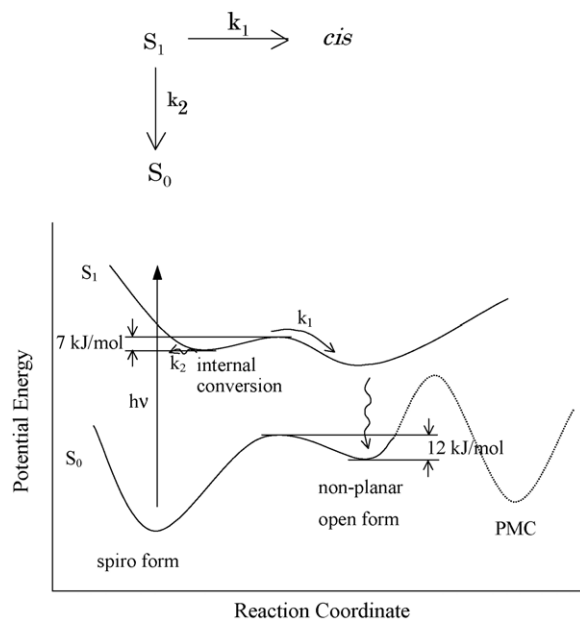


Fig. 8. Scheme and potential curve for the ring-opening reaction according to model B (see text).

conformational change, i.e. the distance between  $C_{\text{spiro}}$  and O atoms, mutual angles of indoline and oxazine rings, and so on.

#### 3.4.1. Model A

The reaction scheme is shown in Fig. 7, where  $[S_0]$ ,  $[S_1]$ ,  $[X]$ , and  $[cis]$  represent the concentration of the  $S_0$  and  $S_1$  state of the spiro form, a short-lived intermediate, and the non-planar open form, respectively. Using the rate constants for each process defined in Fig. 7, the rate equations of  $[S_0]$ ,  $[S_1]$ ,  $[X]$ , and  $[cis]$  are given as

$$\frac{d[S_1]}{dt} = -k_1[S_1] \quad (6)$$

$$\frac{d[X]}{dt} = k_1[S_1] - k_2[X] - k_3[X] \quad (7)$$

$$\frac{d[cis]}{dt} = k_3[X] \quad (8)$$

$$\frac{d[S_0]}{dt} = k_2[X] \quad (9)$$

We ignore here the ring-closure reaction of the non-planar form because it is much slower than the other processes, and assume that the  $S_1$  state decays only through the ring-opening reaction. From these rate equations,  $[cis]$  can be represented by the following equation:

$$[cis] = \frac{k_1 k_3 [S_1]_0}{k_1 - (k_2 + k_3)} \left[ \frac{1 - \exp\{-(k_2 + k_3)t\}}{k_2 + k_3} - \frac{1 - \exp(-k_1 t)}{k_1} \right] \quad (10)$$

Therefore, the yield of the non-planar form is represented by

$$\Phi = \frac{k_1 k_3 [S_1]_0}{k_1 - (k_2 + k_3)} \left( \frac{1}{k_2 + k_3} - \frac{1}{k_1} \right) \quad (11)$$

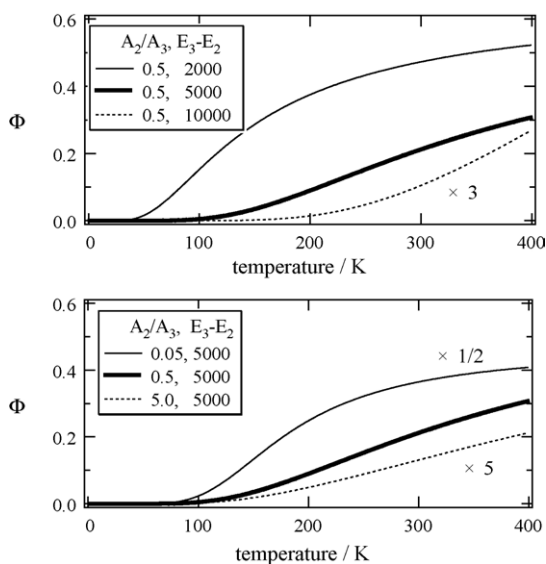


Fig. 9. Calculated temperature dependence of the yield of the non-planar open form on the bases of Model A, using Eq. (13) for several values of  $A_2/A_3$  and  $E_3 - E_2$ .

$$\Phi \cong \frac{k_3}{k_2 + k_3} \quad (12)$$

Because the short-lived intermediate X was not observed directly in the transient absorption measurement, we set  $k_3, k_2 \gg k_1$  and simplify Eq. (11) into Eq. (12). By assuming the Arrhenius type temperature dependence for  $X \rightarrow S_0$  and  $X \rightarrow \text{cis}$ , Eq. (12) can be rewritten to

$$\Phi = \frac{1}{1 + \frac{A_2}{A_3} \exp\left(-\frac{E_2 - E_3}{RT}\right)} \quad (13)$$

$A_2, A_3, E_2$ , and  $E_3$  represent frequency factors and activation energies for each process, respectively. Fig. 9 shows the calculation results of  $\Phi$  using Eq. (13) for several values of  $A_2/A_3$  and  $E_3 - E_2$ . The calculated  $\Phi$  shows an almost linear relation to the temperature in the region of 100–400 K, when the value of  $E_3 - E_2$  is about 5 kJ mol<sup>-1</sup>. A smaller value of  $E_3 - E_2$  leads to a linear increase of  $\Phi$  in a lower temperature range and a saturation behavior in a high temperature region, while for the larger value,  $\Phi$  increase super-linearly with temperature above 200 K. The similar behavior is observed for changing the value of  $A_2/A_3$ .

On the other hand, the experimental result on  $\Phi$  in Fig. 5 shows a linear temperature dependence in the range from 140 to 360 K, which is quantitatively similar to the calculated one using  $A_2/A_3 = 0.5$  and  $E_3 - E_2 = 5$  kJ mol<sup>-1</sup>. Therefore, we consider that model A is a probable reaction mechanism for explaining the present result. A short-lived intermediate, X, is generated before the non-planar open form which lived over several hundreds ps, and will return to the ground state of the spiro form in competitive with changing to the non-planar form. Because the experimental result of Yield is a relative yield of the non-planar open form, we cannot estimate the absolute values of  $A_2, A_3, E_2$ , and  $E_3$ . However, the numerical calculations in Fig. 9 suggest strongly that the activation energy of  $X \rightarrow S_0$  is larger than that of  $X \rightarrow \text{cis}$

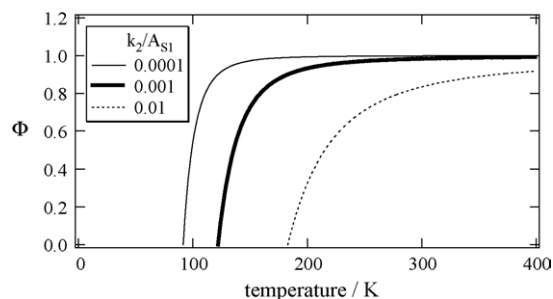


Fig. 10. Calculated temperature dependence of the yield of the non-planar open form on the bases of Model B.

and the frequency factors of the two processes are comparable to each other. So, it is considered that the yield of the non-planar open form will be small in crystal even at a high temperature.

### 3.4.2. Model B

The rate equations for [S0], [S1], and [cis] in case of model B are given by

$$\frac{d[S1]}{dt} = -k_1[S1] - k_2[S1] \quad (14)$$

$$\frac{d[\text{cis}]}{dt} = k_1[S1] \quad (15)$$

$$\frac{d[S0]}{dt} = k_2[S1] \quad (16)$$

And  $\Phi$  can be represented by

$$\Phi = \frac{k_1}{k_1 + k_2} \quad (17)$$

$$\Phi = k_1 \tau_{S1} \quad (18)$$

where

$$\tau_{S1} = \frac{1}{k_1 + k_2} \quad (19)$$

$$k_1 = \frac{1}{\tau_{S1}} - k_2 \quad (20)$$

By assuming  $k_2$  is independent of temperature, Eq. (18) can be rewritten to

$$\Phi = \left(\frac{1}{\tau_{S1}} - k_2\right) \tau_{S1} = 1 - k_2 \tau_{S1} = 1 - \frac{k_2}{A_{S1}} \exp\left(\frac{E_{S1}}{RT}\right) \quad (21)$$

Fig. 10 shows the calculated temperature dependence by Eq. (21) for several values of  $k_2$ , using the experimental values of  $A_{S1} = 5.3 \times 10^{12}$  s<sup>-1</sup> and  $E_{S1} = 7$  kJ mol<sup>-1</sup>. The calculated result based on model B is clearly disagrees with the experimental result as far as assuming the temperature-independent  $k_2$ . To obtain a linear temperature dependence of  $\Phi$  above certain temperature by using Eq. (21), one may assume a negative temperature dependence of  $k_2$ , i.e.  $k_2$  increases with decreasing of temperature. However, in general non-radiative decay of aromatic compounds became slower at lower temperature. Then, we can conclude that the observed temperature dependence cannot be explained by this reaction model.

#### 4. Conclusion

We measured the transient absorption spectra of spiro-phthoxazine microcrystalline powder and investigated the temperature dependence of the lifetimes of the  $S_1$  state of the spiro form and the non-planar open form. The ring-opening in the  $S_1$  state occurred in a picosecond time scale and ring-closure reaction of the open form in a nanosecond time scale. Both reactions exhibited Arrhenius type temperature dependence with activation energy of 7 and 12 kJ mol<sup>-1</sup>, respectively. The molecular structural change for the C–O bond breaking will be strongly restricted in crystalline phase, while after the bond breaking an unstable non-planar conformation of the open form is trapped in crystalline lattice in a nanosecond time scale. On the other hand, the relative yield of the non-planar open form decreased drastically with decreasing temperature. Kinetic analysis of the temperature dependences indicate strongly that the non-planar form with a nanosecond lifetime is not generated directly after the C–O bond breaking in the  $S_1$  state. A short-lived species having a molecular conformation different from the non-planar form should be considered as an intermediate in the ring-opening reaction.

#### References

- [1] G.H. Brown, Photochromism, Wiley–Interscience, New York, 1971.
- [2] H. Dürr, H.B. Laurent, Photochromism: Molecules and Systems, Elsevier, Amsterdam, 1990.
- [3] J.C. Crano, R. Gugliemetti, Organic Photochromic and Thermochromic Compounds, vol. 1 and 2, Plenum Press, New York, 1999.
- [4] N.P. Ernsting, T.A. Engeland, J. Phys. Chem. 95 (1991) 5502.
- [5] N. Tamai, H. Masuhara, Chem. Phys. Lett. 191 (1991) 189.
- [6] N. Tamai, H. Miyasaka, Chem. Rev. 100 (2000) 1875, and references there in.
- [7] T. Asahi, H. Masuhara, Chem. Lett. (1997) 1165.
- [8] M. Suzuki, T. Asahi, H. Masuhara, Mol. Cryst. Liq. Cryst. 345 (2000) 51.
- [9] M. Suzuki, T. Asahi, H. Masuhara, Phys. Chem. Chem. Phys. 4 (2002) 185.
- [10] T. Asahi, M. Suzuki, H. Masuhara, J. Phys. Chem. A 106 (2002) 2335.
- [11] M. Suzuki, T. Asahi, H. Masuhara, Chem. Phys. Lett. 368 (2003) 384.
- [12] T. Asahi, A. Furube, H. Fukumura, M. Ichikawa, H. Masuhara, Rev. Sci. Instrum. 69 (1998) 361.
- [13] T. Asahi, Y. Matsuo, H. Masuhara, Chem. Phys. Lett. 256 (1996) 525.
- [14] A. Zelichenok, F. Buchholtz, J. Ratner, E. Fischer, V. Krongauz, J. Photochem. Photobiol. A: Chem. 77 (1994) 201.